# Link between liquid structure and the nucleation barrier for icosahedral quasicrystal, polytetrahedral, and simple crystalline phases in Ti-Zr-Ni alloys: Verification of Frank's hypothesis

G. W. Lee,[1,*] A. K. Gangopadhyay,[1] T. K. Croat,[1] T. J. Rathz,[2] R. W. Hyers,[3] J. R. Rogers,[4] and K. F. Kelton[1]
[1]*Department of Physics, Washington University and the Center for Materials Innovation, St. Louis, Missouri 63130, USA*
[2]*University of Alabama, Huntsville, Alabama 35801, USA*
[3]*University of Massachusetts, Amherst, Massachusetts 01003, USA*
[4]*NASA Marshall Space Flight Center, Huntsville, Alabama 35812, USA*
(Received 15 July 2005; published 8 November 2005)

Comprehensive undercooling experiments on a large number of simple crystalline, polytetrahedral, and icosahedral quasicrystalline phase forming compositions in Ti-Zr-Ni alloys have been carried out using electrostatic levitation (ESL) techniques for containerless processing. Consistent with Frank's hypothesis, a direct correlation was found between the reduced undercooling $[\Delta T_r=(T_l-T_r)/T_l$, where $T_r$ and $T_l$ are the nucleation and liquidus temperatures, respectively] and the icosahedral short-range order in the solid. The reduced undercooling is less for liquids that form the icosahedral quasicrystal (*i* phase) than for those that form the hcp *C*14 Laves polytetrahedral phase. For many compositions near 21 at. % Ni, the primary nucleation of a metastable *i* phase instead of a stable *C*14 Laves phase demonstrates that the interfacial free energy between the liquid and the *i* phase is smaller than between the liquid and the *C*14 Laves phase, indicating icosahedral local order in the undercooled liquid. This is in agreement with a classical-nucleation-theory-based estimate of the interfacial free energy and the work of formation of the critical cluster from the undercooling data. Taken together with high-energy x-ray diffraction studies of the undercooled liquid, these results demonstrate that the local structure of liquids in Ti-Zr-Ni alloys is icosahedral, as postulated by Frank over a half century ago.

DOI: 10.1103/PhysRevB.72.174107 PACS number(s): 64.60.Qb, 61.44.Br, 82.60.Nh, 68.03.Cd

## I. INTRODUCTION

Following pioneering work by Turnbull,[1] years of research[2] has established that if heterogeneous nucleation can be avoided, metallic alloy liquids can be maintained in a metastable (undercooled) liquid state, typically down to about 20% of their equilibrium melting temperatures $T_m$. These results demonstrate the existence of an energy barrier for the nucleation of the solid phase from the liquid phase. Frank[3] suggested that the barrier is present because the structure of undercooled metallic liquids is dominated by icosahedral short-range order (ISRO), which is incompatible with the long-range periodicity of a crystalline solid. Although supported by molecular dynamics simulation studies,[4–6] the direct experimental verification of this hypothesis is difficult. The recent developments of containerless processing techniques, such as electrostatic,[7] electromagnetic,[8] aerodynamic,[9] and acoustic[10] levitation, have made it possible to study a wide variety of materials in the undercooled state. The absence of container walls (usual sites for heterogeneous nucleation) is a significant advantage over older methods, such as the emulsification of droplets, for the study of homogeneous nucleation in highly reactive, high-temperature materials.

If, as Frank hypothesized, the nucleation barrier is a consequence of the ISRO in the liquid, the barrier should be smaller for the formation of icosahedral quasicrystals (*i* phase) than for the nucleation of simple crystalline phases. This was first demonstrated[11] in nucleation studies of the icosahedral quasicrystalline phase (henceforth referred to as the *i* phase) during the crystallization of an $Al_{75}Cu_{15}V_{10}$ metallic glass, whose structure was also dominated by ISRO. The interfacial energy ($0.002 \leqslant \sigma \leqslant 0.015$ J/m$^2$) determined was at least an order of magnitude smaller than for simple crystal-liquid interfaces (0.15–0.2 J/m$^2$ for Al and its melt).[2] In further support, undercooling studies of Al-based liquids made using electromagnetic levitation (EML) showed a systematic decrease in the reduced undercooling $[\Delta T_r=(T_l-T_r)/T_l$, where $T_r$ and $T_l$ (in degree K) are the nucleation and liquidus temperatures, respectively] with an increasing degree of icosahedral short-range order in the nucleating solid phase, demonstrating a decreasing nucleation barrier.[12] Frequently, polytetrahedral phases form near the *i*-phase composition;[13–15] some of these (such as the Frank-Kasper phases) also nucleate easily during undercooling and casting experiments.[16,17] Recently, for example an extremely low interfacial energy (0.0008–0.002 J/m$^2$) for nucleation was reported for a Frank-Kasper polytetrahedral phase forming alloy ($MgZn_2$-*C*14 Laves phase),[18] raising the question of whether the local structure of the liquid is actually icosahedral, as Frank proposed, or is polytetrahedral.

For Ti-Zr-Ni alloys containing 21 at. % Ni and a nearly equal Ti to Zr ratio, the nucleation of the *i* phase competes with that of the polytetrahedral phase (*C*14 Laves phase).[19,20] Determinations of the Ti-Zr-Ni phase diagram,[21,22] have revealed an interesting dependence of phase complexity on the Ni concentration, from simple bcc and hcp solid solution phases, to the polytetrahedral *C*14 Laves (hcp) phase, and to quasicrystals and high-order rational approximants. This system, then, provides a unique opportunity to study nucleation of different crystalline and quasicrystalline phases with vary-

 

ing degree of ISRO as a function of composition in the same alloy system.

Recently, by correlating the phase selection in undercooled Ti-Zr-Ni liquids with *in situ* high-energy synchrotron structural studies of the liquid, we demonstrated that the local structure of the liquid was icosahedral, not polytetrahedral.[20] Here, we present a detailed study of the undercooling behavior for a series of Ti-Zr-Ni alloy liquids, using an electrostatic levitation technique; a preliminary report was presented earlier.[21] A clear correlation between $\Delta T_r$ and the ISRO of the nucleating phase is observed. An analysis of the undercooling data using the classical theory of nucleation reveals a systematic decrease in the work for critical cluster formation with increasing ISRO of the ordered phases, supporting Frank's hypothesis.

The paper is organized as follows. Following a brief description of the experimental procedure in Sec. II, undercooling experiments for different crystalline and quasicrystalline phases are presented in Sec. III. The main conclusions from the experimental data are presented in Sec. IV, followed by its analysis in terms of the classical nucleation theory, pointing out some of its limitations. Section V summarizes the main results of this investigation.

## II. EXPERIMENTS

Alloys were prepared by arc melting high-purity elemental Ti (99.995%), Zr (99.95%, 3% Hf), and Ni (99.995%) in a water-cooled Cu hearth under a high-purity argon atmosphere. Undercooling studies were made on small spheres (2.2–2.5 mm diameter) that were prepared from larger ingots by arc melting. For electrostatic levitation, the samples were positively charged with ultraviolet light and levitated by a dc electric field applied between two electrodes under high vacuum ($\approx 10^{-7}$ Torr), as described elsewhere.[7] The samples were melted using a 30 W diode laser and/or a 30 W $CO_2$ laser. To achieve maximum undercooling, it was often necessary to heat the samples to between 100 and 400 °C above the liquidus temperature, presumably to dissolve impurities acting as heterogeneous nucleation sites. Because of the containerless processing and the high-vacuum environment, when the heating lasers were turned off, the samples cooled by radiation alone. Optical pyrometers (Mikron, Infrared) with a 1.45–1.8 $\mu$m wavelength range were used to measure the sample temperature (relative accuracy of ±1 °C) as a function of time during free radiative cooling. Structural and compositional information for each alloy was obtained by x-ray powder diffraction using Cu $K\alpha$ radiation, by transmission electron microscopy using a JEOL 2000FX TEM, and scanning electron microscopy (SEM) using a Hitachi S-4500 SEM equipped with a backscattered electron detector. In a few select cases, *in situ* phase identification was made by synchrotron x-ray diffraction studies of levitated droplets using the recently developed BESL beamline electrostatic levitation (BESL) technique.[23]

## III. EXPERIMENTAL RESULTS

### A. Phase diagram study

A detailed knowledge of the phase diagram is necessary to understand the ordered phase formation sequence from the undercooled liquids. The Ti—Zr—Ni phase diagram has been studied extensively by our group over the past decade;[21,22] a section of that ternary diagram for an equal ratio of Ti and Zr is shown in Fig. 1. For low Ni compositions (≤5 at. %), the primary crystallizing phase is $\beta$(Ti/Zr), a bcc solid solution phase, which transforms into the $\alpha$(Ti/Zr) hcp solid solution phase at lower temperatures. The $MgZn_2$-type $C14$ Laves phase occurs in alloys containing higher Ni (≥22 at. %) concentrations. In between, over a narrow concentration range (16≤Ni≤18 at. %), the $i$ phase (with quasilattice constant $a_q$=0.51 nm) and a related 1/1 rational approximant phase (bcc type with a lattice constant $a$=1.43 nm) form at lower temperatures (≈570–600 °C) from a high-temperature mixture of the $\beta$ and Laves phases. The present work focuses on the nucleation of these crystalline and quasicrystalline phases from the undercooled melt over a wide composition range. It is apparent that since the phase boundary of the $i$ phase (Ni 17 at. %) does not extend to the liquidus temperatures, and since the nucleation barrier of the $C14$ phase is low, it is unlikely for the $i$ phase to nucleate directly from the undercooled liquid. However, we will show in Sec. III B 2 that over a narrow concentration range around 21 at. % Ni, the nucleation of a metastable $i$ phase is preferred over that of the stable $C14$ Laves phase, reflecting the lower nucleation barrier and the more similar local structures of the liquid and the $i$ phases.

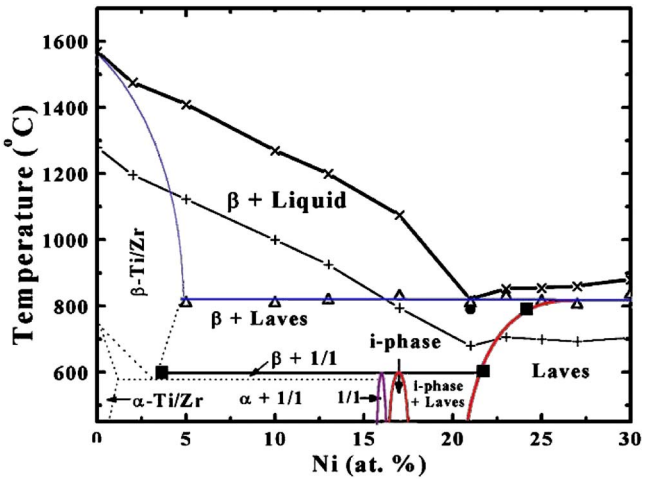


FIG. 1. (Color online) Vertical section of the phase diagram of Ti-Zr-Ni alloys for an equal ratio of Ti and Zr. The liquidus (×) temperatures were determined by ESL measurements. The eutectic temperature (△) and the solid-phase boundaries (■) were determined by long annealing treatments of as-cast samples; (●) indicates the metastable solidus temperature of the $i$ phase, determined from nucleation studies in ESL of 21 at. % Ni samples. The maximum undercooling temperatures as a function of Ni concentration are also shown (+).

### B. Undercooling studies of Ti-Zr-Ni alloys

In this section, the results of undercooling studies as a function of concentration for Ti-Zr-Ni liquids are presented. For presentation, the studies are divided into subsections that correspond to the different primary crystallizing phases.

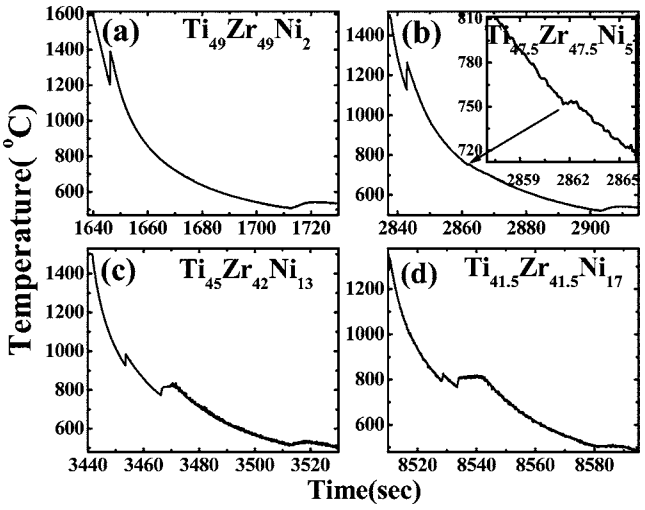


FIG. 2. Temperature-time cooling curves for ESL-processed Ti-Zr-Ni alloy liquids for low Ni concentrations that nucleate $\beta$(Ti/Zr) as the primary crystallizing phase.

#### *1. Undercooling behavior of liquids forming the $\beta$(Ti/Zr) solid solution phase*

As already discussed, if the local structure of the liquid is icosahedral, a large undercooling is expected for the primary crystallization of simple crystalline phases such as $\beta$(Ti/Zr). Figures 2(a)–2(d) show the measured temperature as a function of time during free radiative cooling in the ESL for some representative Ti-Zr-Ni alloy liquids that nucleate $\beta$(Ti/Zr).

The nucleation and fast growth of a solid from the undercooled liquid is marked by an almost adiabatic rise in temperature, called the recalescence, due to the large latent heat release. Only one recalescence event is observed for the alloy containing 2 at. % Ni [Fig. 2(a)], as expected from the equilibrium phase diagram. The onset temperature at approximately 1200 °C is due to the nucleation and growth of $\beta$(Ti/Zr), the only stable phase that forms for this composition. Another small recalescence at approximately 550 °C is due to the solid state transformation of $\beta$(Ti/Zr) to $\alpha$(Ti/Zr). The presence of only the $\alpha$ phase in the x-ray diffraction patterns [Fig. 3(a)] and the single-phase microstructure in the SEM (not shown) of the ESL-processed sample confirms the primary crystallization of $\beta$(Ti/Zr) from the undercooled liquid in this alloy. In addition to the high-temperature recalescence, the $Ti_{47.5}Zr_{47.5}Ni_5$ alloy shows a small plateau near 750 °C [see the inset of Fig. 2(b)] indicative of the formation of the $C14$ Laves phase from the remainder of the liquid. This second recalescence becomes increasingly more prominent with increasing Ni, such as for the 13 and 17 at. % Ni samples, with a corresponding decrease in the magnitude of the higher-temperature recalescence. This reflects the decrease in the volume fraction of $\beta$(Ti/Zr) that forms and an increase in the amount of the $C14$ phase as the Ni concentration is increased, consistent with the equilibrium phase diagram (Fig. 1). The proposed phase formation sequence was confirmed by x-ray diffraction and scanning electron microscopy studies of ESL-processed samples (Fig. 3). Based on energy-dispersive x-ray spectroscopy, the lighter grains observed in Fig. 3(b) correspond to the Ni-poor solid solution phase, $\alpha$(Ti/Zr), and the darker grains are the Ni-rich $C14$ phase. The sign of curvature of the solid solution phase boundaries indicate that $\beta$(Ti/Zr) nucleated from the liquid during the first recalescence (primary crystallization), followed by the nucleation and growth of the Laves phase from the rest of the liquid during the second recalescence. As listed in Table I, the typical reduced undercooling for $\beta$(Ti/Zr), $\Delta T_r = 0.18$, is large (bcc), as expected. As shown in Fig. 1, the recalescence temperature (+) decreases with increasing Ni concentration, approximately paralleling the liquidus temperature (×).

#### *2. Undercooling of the i-phase-forming liquids*

Undercooling studies of a large number of alloys (Table I) containing 13–17 at. % Ni showed that $\beta$(Ti/Zr) and the $C14$ phases, the expected high-temperature phases, nucleated from the liquid. Interestingly, the recalescence behavior for the 21 at. % Ni alloys is different. Instead of the two sequential recalescences for the alloys containing less than 20 at. % Ni, a two-step recalescence was observed, as shown in Fig. 4. A plateau of a few seconds duration at 790 °C occurs after the first recalescence, but progresses to a second rise in temperature and another plateau at 810 °C, corresponding to the eutectic temperature; the liquidus temperature is about 820 °C. Interestingly, the time duration of the plateau after the first recalescence decreases as the alloy concentration is shifted away from $Ti_{37}Zr_{42}Ni_{21}$, indicating a decrease in the volume fraction of the primary crystallizing phase. While the Ni concentration is critical for the occurrence of this two-

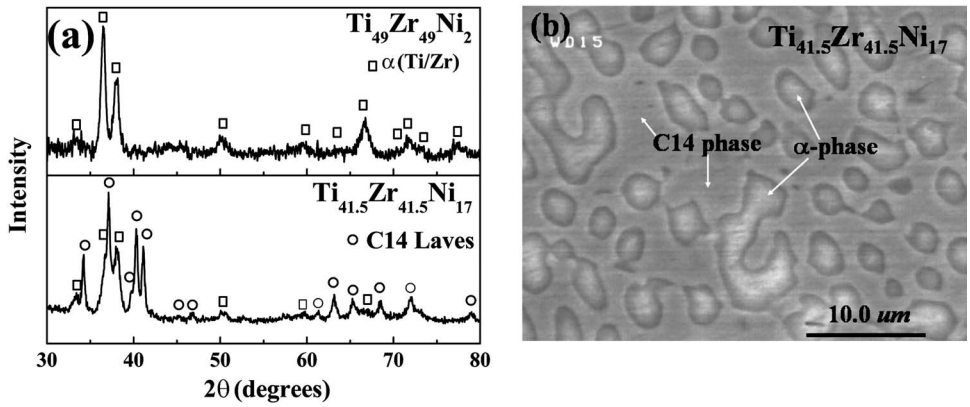


FIG. 3. (a) X-ray diffraction for low-Ni-concentration alloys showing $\alpha$ solid solution (□) and $C14$ Laves phase (○). (b) Backscatter SEM micrograph of $Ti_{41.5}Zr_{41.5}Ni_{17}$.

TABLE I. Reduced undercooling data for Ti-Zr-Ni alloys, correlated with the primary crystallizing phase ($T_s$, $T_l$, $T_{r1}$, $T_{r2}$, are the solidus, liquidus, first, and second recalescence temperatures, respectively).

| Compositions (Ti-Zr-Ni) | $T_s$ (°C) | $T_l$ (°C) | $T_{r1}$, $T_{r2}$ (°C) | $\Delta T=T_l-T_r$ | $\Delta T_r=\Delta T/T_l$ | Average value of $\Delta T_r$ | Primary phase | Other phases present in the ESL-processed samples |
|---|---|---|---|---|---|---|---|---|
| 50-50-0 | | 1570 | 1280 | 290 | 0.157 | 0.181±0.014 (solid solution) | $\beta$ | $\beta$ |
| 49-49-2 | | 1476 | 1196 | 280 | 0.16 | | $\beta$ | $\beta$ |
| 47.5-47.5-5 | 810 | 1410 | 1123 | 287 | 0.171 | | $\beta$ | *C*14 |
| 45-45-10 | 810 | 1270 | 1000 | 270 | 0.174 | | $\beta$ | *C*14 |
| 20-67-13 | 811 | ~1315 | 1018, 699 | 297 | 0.187 | | $\beta$ | $Zr_2Ni$ |
| 37-50-13 | 803 | ~1225 | 941, 766 | 284 | 0.189 | | $\beta$ | *C*14 |
| 45-42-13 | 818 | ~1200 | 926, 774 | 274 | 0.186 | | $\beta$ | *C*14 |
| 33-50-17 | 800 | ~1075 | 834, 760 | 241 | 0.178 | | $\beta$ | *C*14 |
| 37-46-17 | 816 | ~1100 | 825, 771 | 275 | 0.20 | | $\beta$ | *C*14 |
| 41-42-17 | 825 | ~1075 | 823, 782 | 252 | 0.186 | | $\beta$ | *C*14 |
| 41.5-41.5-17 | 830 | ~1075 | 795, 767 | 280 | 0.207 | | $\beta$ | *C*14 |
| 45-38-17 | 831 | ~1060 | 820, 788 | 240 | 0.18 | | $\beta$ | *C*14 |
| 50-33-17 | 836 | ~1070 | 828, 793 | 242 | 0.18 | | $\beta$ | *C*14 |
| 60-23-17 | 846 | ~1100 | 856, 806 | 244 | 0.177 | | $\beta$ | *C*14 |
| 25-54-21 | 796 | 811 | 729 | 82 | 0.075 | | # | $Zr_2Ni$, $\beta$ *C*14 |
| 29-50-21 | 784 | 820 | 730 (762) | 53 | 0.082 | | | |
| 33-46-21 | 792 | 811 | 693 (774) | 81[a] | 0.08 | 0.093±0.008 (*i* phase) | *I* | $\beta$, *C*14 |
| 37-42-21(STL212) | 803 | 820 | 681 (786) | 105[a] | 0.1 | | *I* | $\beta$, *C*14 |
| 37-42-21(STL127) | 808 | 827 | 696 (789) | 93[a] | 0.09 | | *I* | $\beta$, *C*14 |
| 39.5-39.5-21 | 810 | 820 | 681 (790) | 109[a] | 0.102 | | *I* | $\beta$, *C*14 |
| 41-38-21 | 823 | 840 | 709 (803) | 94[a] | 0.09 | | *I* | $\beta$, *C*14 |
| 45-34-21 | 835 | 845 | 706 (810) | 104[a] | 0.096 | | *I* | $\beta$, *C*14 |
| 50-29-21 | 845 | 852 | 715 | 137 | 0.121 | | | |
| 55-24-21 | 845 | 850 | 754 | 96 | 0.085 | | | |
| 38.5-38.5-23 | 830 | 853 | 707 | 146 | 0.129 | | *C*14 | $\beta$ |
| 15-60-25 | 790 | 894 | 679 | 215 | 0.184 | 0.154±0.022 ($Zr_2Ni$) | $Zr_2Ni$ | $\beta$ |
| 25-50-25 | 796 | 800 | 655 | 145 | 0.135 | | $Zr_2Ni$ | $\beta$, *C*14 |
| 33-42-25 | 793 | 840 | 680 | 160 | 0.143 | 0.142±0.009 (*C*14 Laves phase) | *C*14 | $\beta$ |
| 37-38-25 | 815 | 855 | 700 | 155 | 0.137 | | *C*14 | $\beta$ |
| 41-34-25 | 844 | 872 | 708 | 164 | 0.143 | | *C*14 | $\beta$ |
| 45-30-25 | 846 | 862 | 710 | 152 | 0.133 | | *C*14 | $\beta$ |
| 55-20-25 | 843 | 856 | 750 | 106 | 0.093 | | *C*14 | $\beta$ |
| 65-10-25 | 844 | 930 | 801 | 129 | 0.107 | | $Ti_2Ni$ | *C*14 |
| 36.5-36.5-27 | 804 | 860 | 694 | 166 | 0.146 | | *C*14 | $Zr_2Ni$ |
| 20-50-30 | 800 | 880 | 717 | 163 | 0.141 | | $Zr_2Ni$ | *C*14 |
| 30-40-30 | 818 | 869 | 690 | 179 | 0.156 | | $Zr_2Ni$ | *C*14 |
| 35-35-30 | 835 | 880 | 705 | 175 | 0.151 | | *C*14 | $Zr_2Ni$ |
| 40-30-30 | 865 | 892 | 730 | 152 | 0.137 | | *C*14 | |
| 50-20-30 | 840 | 890 | 747 | 143 | 0.123 | | $Ti_2Ni$ | *C*14 |
| 40-27-33 | 911 | 921 | 734 | 187 | 0.156 | | *C*14 | |

[a]From the melting temperature of the metastable *i* phase.

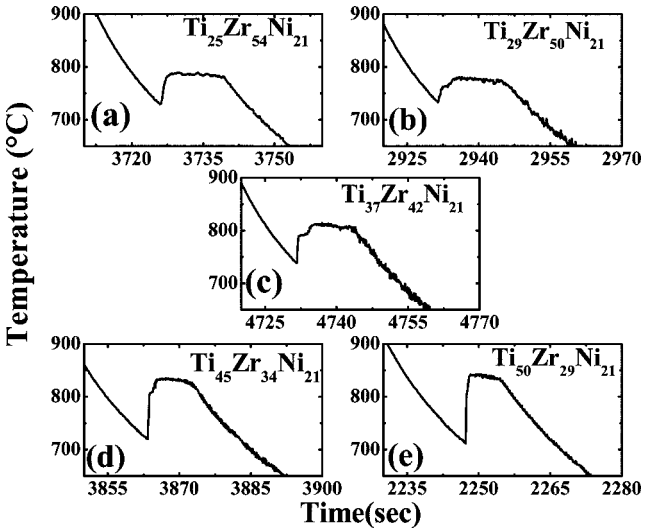


FIG. 4. Two-step recalescence for the alloys containing 21 at. % Ni and different Ti to Zr ratio. The two steps merge into one in (a) and (e).

step recalescence ($20.5 \leqslant \mathrm{Ni} \leqslant 21.5$ at. %), the Ti and Zr concentration ratio is less critical ($29 \leqslant \mathrm{Ti} \leqslant 45$ at. %) (Table I and Fig. 4). A rod eutectic microstructure, consisting of $\alpha$(Ti/Zr) and the $C14$ phase, is obtained after ESL processing [cf Fig. 7(b)].

It might appear that the first recalescence could correspond to the nucleation of $\beta$(Ti/Zr) and the second, to the $C14$ phase, or vice versa. However, if $\beta$(Ti/Zr) nucleated first, the reduced undercooling ($\Delta T_r = 0.09$) and the solidus temperature (plateau temperature, ~790 °C) would be smaller than those for the $C14$ phase (Table I). If the $C14$ phase nucleated first, the solidus temperature would be smaller than the eutectic temperature in the phase diagram. The two-step recalescence is, therefore, characteristic of the nucleation of a metastable phase, followed by the nucleation of the stable phase or phase mixture. This is supported by a comparison of the nucleation behavior of the *i phase-forming* liquids at different levels of undercooling. Figure 5 shows the recalescence behavior of a $Ti_{37}Zr_{42}Ni_{21}$ alloy liquid held at two different undercooled temperatures. When held at 780 °C (small, 40 °C undercooling), just below the highest plateau temperature, the undercooled liquid shows only one recalescence [Fig. 5(a)]. On the other hand, when held at lower temperatures (680 to 760 °C, deeper undercooling), a two-step recalescence is observed [Fig. 5(b)].

A recent study[19] showed that an almost single-phase $i$ phase was formed in small (0.05 g) cast ingots of this alloy, while a mixture of $\alpha$(Ti/Zr) and the $C14$ phase were obtained in large cast ingots, suggesting that the $i$ phase is metastable at high temperatures and can be retained only by fast cooling (smaller ingot). This is an indication that the lower-temperature recalescence in the ESL data corresponds to the formation of a metastable $i$ phase. Unambiguous evidence for this was obtained by recent *in situ* identification of the recalescing phases by fast, high-energy synchrotron x-ray diffraction studies using the beamline electrostatic levitator.[20,23] The metastable (at the recalescence temperature) $i$ phase nucleates directly from the undercooled liquid during the first recalescence, and decomposes to the $\beta$(Ti/Zr) and $C14$ phases during the second recalescence. The average reduced undercooling measured for different $i$-phase-forming liquids was 0.09 (Table I), much smaller than that for the polytetrahedral $C14$, and the simple crystalline $\beta$ phases, as expected from Frank's hypothesis.

### 3. *Undercooling of the polytetrahedral C14 Laves– and $Zr_2Ni$-phase-forming liquids*

Liquids containing 25 at. % and higher Ni show one recalescence event [Figs. 6(b)–6(f)], compared to the two-step recalescence for the 21 at. % Ni alloy [Fig. 6(a)]. X-ray diffraction [Fig. 7(a)] and SEM studies (not shown) on these ESL-processed samples indicate that they contain primarily the $C14$ phase, with only a small volume fraction of $\alpha$(Ti/Zr); for $Ti_{40}Zr_{30}Ni_{30}$ and $Ti_{40}Zr_{27}Ni_{33}$ alloys, only the $C14$ phase was detected. These data indicate that the $C14$ phase nucleated directly from these undercooled liquids. The average reduced undercooling for this polytetrahedral phase is about 0.14 (see Table I), which is smaller than for liquids that form $\beta$(Ti/Zr), but larger than for those that form the $i$ phase, in agreement with the expectations from Frank's hypothesis for a liquid with significant ISRO.

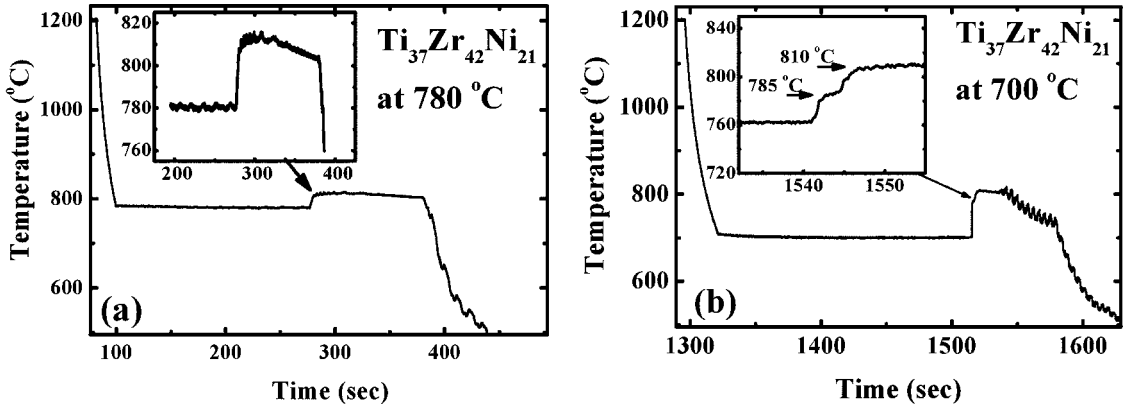


FIG. 5. Recalescence behavior for different levels of undercooling for a $Ti_{37}Zr_{42}Ni_{21}$ alloy. While small undercooling [780 °C, (a)] shows one recalescence, deep undercoolings [760 °C, inset of (b), and 700 °C (b)] show two-step recalescences.

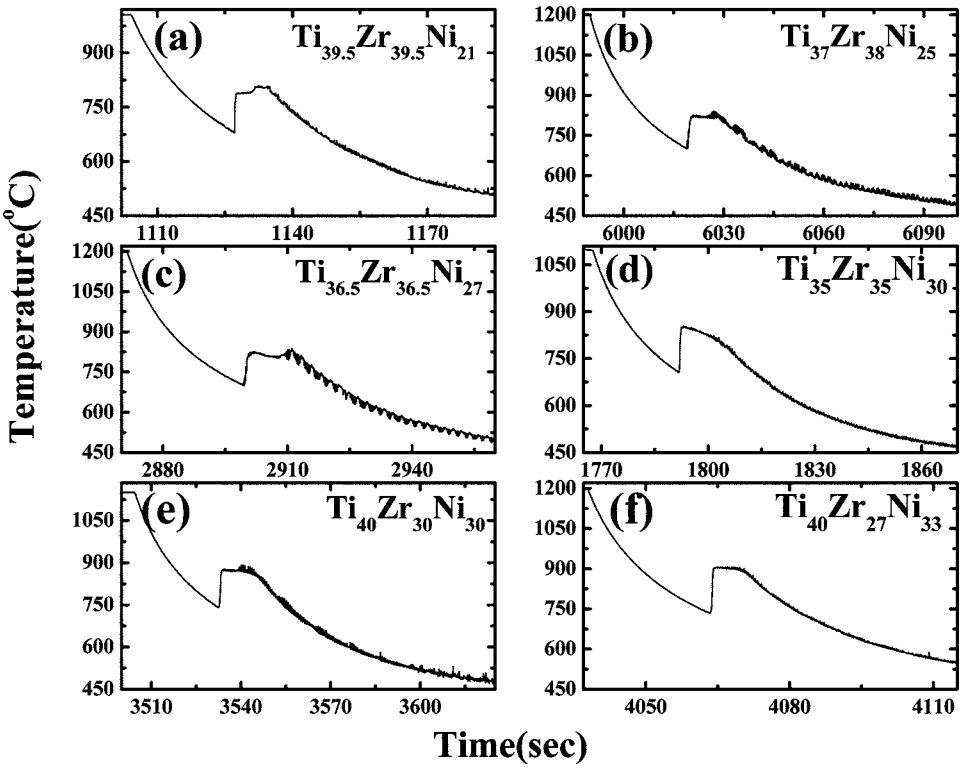


FIG. 6. Temperature-time cooling curves for ESL-processed Ti-Zr-Ni alloy liquids containing higher ($\geqslant$21 at. %) Ni concentrations.

For some Zr-rich compositions (Table I) containing 25 at. % and higher Ni, the primary crystallizing phase is $Zr_2Ni$. The reduced undercooling (0.154) for this phase is larger than for the $C14$ Laves phase but smaller than for the $\beta$(Ti/Zr) phase, consistent with the above expectation.

## IV. DISCUSSION

### A. Summary of undercooling data: relation between ISRO and undercooling

The undercooling data for all Ti-Zr-Ni alloys studied are summarized in Table I. To illustrate the main results of this study, the reduced undercooling values for a few select alloys with an equal Ti-to-Zr ratio are plotted as a function of Ni concentration in Fig. 8. The primary conclusion is

$$\Delta T_r(i \text{ phase}) < \Delta T_r(C14 \text{ Laves and } Zr_2Ni \text{ phases}) < \Delta T_r(\beta \text{ phase}).$$

This result is consistent with earlier EML undercooling studies of Al-based alloys,[24] and provides support for Frank's hypothesis. A more detailed interpretation in terms of the nucleation barrier is provided in Sec. IV B

The recalescence temperature $T_r$ for $\beta$(Ti/Zr) decreases with increasing Ni, following the behavior of the liquidus temperature $T_l$ (Fig. 1). Since $\Delta T$ ($=T_l-T_r$) does not change significantly over this concentration range (Table I), the increase in the reduced undercooling $[\Delta T_r=(T_l-T_r)/T_l]$ observed in Fig. 8 is largely due to the decreasing $T_l$. Similar results were also reported for Pb-Sb alloys.[25]

This trend breaks down near 21 at. % Ni, when a sudden drop in the reduced undercooling marks the nucleation and

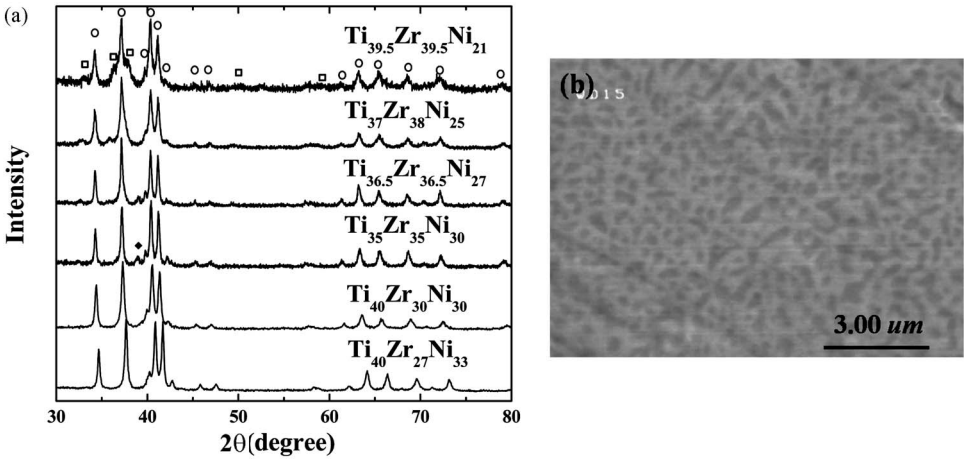


FIG. 7. (a) X-ray powder diffraction patterns for alloys containing between 21 and 33 at. % Ni after ESL processing [○, $C14$ phase; □, $\alpha$(Ti/Zr)-phase; and ◆, $(Zr/Ti)_2Ni$]. (b) Backscatter SEM micrograph of a $Ti_{39.5}Zr_{39.5}Ni_{21}$ alloy showing the rod eutectic microstructure.

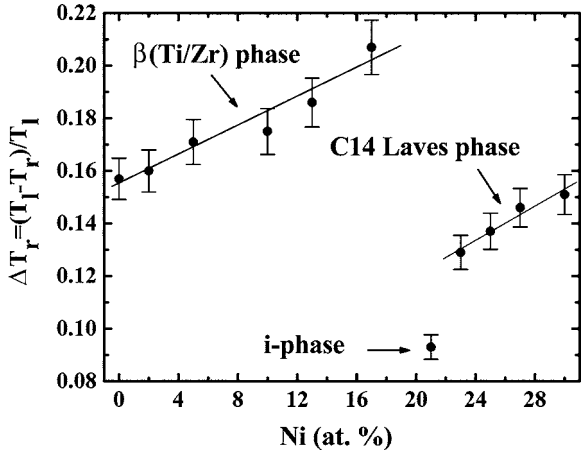


FIG. 8. Reduced undercooling for Ti—Zr—Ni liquids as a function of Ni concentration ([Ti]/[Zr]=1); the solid lines are a guide to the eye.

growth of the metastable *i* phase from the undercooled liquid; this is due to a developing ISRO in the liquid (see Sec. IV C and Ref. 20). The structure of the Ti-Zr-Ni *i* phase is dominated by a 45-atom cluster (Bergman cluster), consisting of an inner icosahedral cluster with a Ni atom at the center and 12 Ti atoms on the vertices, and an outer cluster with 12 Ni atoms on the vertices and 20 Zr atoms on the faces.[26–28] Results of a synchrotron x-ray diffraction experiment on an electrostatically levitated $Ti_{39.5}Zr_{39.5}Ni_{21}$ liquid,[20] were described by assuming that the local structure in the liquid is dominated by the inner-shell icosahedron from the *i* phase structure. This well-defined ISRO in the liquid favored the nucleation of a metastable *i* phase instead of competing stable phases[20] (Laves phase and $\beta$ phase) due to the lower nucleation barrier.

In the absence of direct measurements of the driving free energy for crystallization for all alloy compositions, the origin of the weak composition dependences of $\Delta T_r$ for the $\beta$(Ti/Zr) and *C*14-forming liquids is unclear. As expected from the classical theory of nucleation, for a composition independent interfacial free energy and heat of fusion, the recalescence temperature for $\beta$(Ti/Zr) decreases with increasing Ni concentration, paralleling the decreasing liquidus temperature. However, since Ni has a strong negative heat of mixing with both Ti and Zr, favorable for the formation of short-range order, it is reasonable to expect that up to some concentration, the addition of Ni enhances the formation of ISRO in the liquid. This is supported by direct measurement of the SRO in these alloy liquids as a function of Ni concentration.[29] In addition to changing the free energy of the liquid phase, this should also increase the interfacial free energy between the liquid and $\beta$(Ti/Zr), contributing to an increase in the work of cluster formation [Eq. (2)] and an increase in $\Delta T_r$ (Sec. IV B).

For higher Ni compositions, as the *C*14 Laves phase becomes the primary nucleating phase, the reduced undercooling increases again, and continues to rise with further increase in Ni concentration (Fig. 8). Unlike the case for $\beta$(Ti/Zr), however, this does not follow the liquidus temperature. Due to the small increase in the liquidus temperature over this composition range (Fig. 1 and Table I), the reduced undercooling should decrease slightly if this were the case. Instead, the increase in $\Delta T_r$ suggests a rising barrier for the nucleation of the *C*14 Laves phase for Ni$>$21 at. %. This may reflect a decrease in the driving free energy and/or an increase in the interfacial free energy for higher Ni compositions, as the SRO of the liquid becomes different from that of the *C*14 Laves phase, which is polytetrahedral or, equivalently, distorted ISRO.[30] The analysis of x-ray diffraction results for these liquids is currently in progress to clarify this point.

### B. Nucleation and interfacial energy

To make the undercooling data more quantitative, the classical theory of nucleation is used to estimate the interfacial free energy between the liquid and the nucleating phases. While the absolute magnitude of the interfacial free energies determined in this way is certainly questionable,[2] a relative comparison of the values should reflect the structural differences between the liquid and the crystallizing phases. Within the classical theory, the steady state nucleation rate per unit volume at temperature $T$ is given by[2]

$$I^s = \frac{6n^{*2/3}k_BTN_A}{\pi\lambda^3\eta(T)}\left(\frac{\delta\mu}{6\pi k_BTn^*}\right)^{1/2}\exp\left(-\frac{W^*}{k_BT}\right) \qquad (1)$$

where $\eta$, $\lambda$, $n^*$, $\delta\mu$, and $W^*$ are the viscosity, the average atomic jump distance, the number of atoms in the critical nucleus, the Gibbs free energy difference between the initial and final phases per atom (driving free energy), and the work of critical cluster formation, respectively; $k_B$ is Boltzmann's constant and $N_A$ is the Avogadro number. $W^*$ is determined by the driving free energy ($\delta\mu$), the interfacial free energy ($\sigma$), and the average atomic volume ($\bar{v}$),

$$W^* = \frac{16\pi}{3}\frac{\sigma^3}{|\delta\mu/\bar{v}|^2}. \qquad (2)$$

Assuming that transient nucleation effects are small,[2] these expressions can be used to compute $\sigma$ from the undercooling data under the assumption that one nucleation event is required to initiate solidification of the undercooled liquid. Therefore, the product of the steady state nucleation rate, sample volume, and the time that the sample remains at the nucleation temperature, should be greater than 1, i.e., $I^s(T_r)Vt_r \geq 1$. The time for the sample at each temperature can be calculated from the free cooling curves. Several approximate expressions for the driving free energy $\Delta G$ ($\delta\mu = \Delta G/N_A$) have been developed from the heat of fusion $\Delta H_f$ and the entropy difference between the liquid and nucleating solid $\Delta S_f$ and the undercooling temperature $\Delta T$ ($=T_l-T_r$). We used the following three expressions[1,31,32] in our calculations:

$$\Delta G = \frac{\Delta H_f\Delta T}{T_l}, \qquad (3a)$$

$$\Delta G = \frac{\Delta H_f\Delta T}{T_l}\frac{2T}{T_l+T}, \qquad (3b)$$

TABLE II. Interfacial free energies ($\sigma$), $\alpha_{LS}=\sigma_g/\Delta H_f$ from Eq. (3a), work for critical cluster formation, and critical radius $r^*$ for the three ($i$, Laves, and $\beta$) phases.

| | $\sigma$ (J/m$^2$) | | | | | | Parameters used | | |
|---|---|---|---|---|---|---|---|---|---|
| Phase | (3a) | (3b) | (3c) | $\alpha_{LS}$ | $W^*/k_BT_r$ | $r^*$ (Å) (at $T_r$) | $\rho$ (g/cm$^3$) | $C_p$ (J/mol K) | $\Delta H_f$ (kJ/mol) |
| $i$ phase | 0.062± | 0.05± | 0.051± | 0.324 | 58.28± | 17.23± | 5.712 | 44.24± | 8.48±0.40 |
| ($Ti_{39.5}Zr_{39.5}Ni_{21}$) | 0.002 | 0.001 | 0.002 | ±0.009 | 0.15 | 0.32 | | 1.54 | |
| $C14$ Laves | 0.095± | 0.086 | 0.089 | 0.375 | 60.68± | 14.38± | 5.448 | 42.45± | 11.2±0.42 |
| ($Ti_{40}Zr_{30}Ni_{30}$) | 0.006 | | | ±0.017 | 0.29 | 0.57 | | 3.78 | |
| Solid solution phase | 0.077± | 0.074 | 0.077 | 0.59 | 61.21± | 19.56± | 5.884 | 33.57± | 6.12±0.13 |
| ($Ti_{49}Zr_{49}Ni_2$) | 0.002 | | | ±0.013 | 0.40 | 0.13 | | 1.65 | |

$$\Delta G = \frac{\Delta H_f \Delta T}{T_l} - \gamma \Delta S_f \left[ \Delta T - T \ln\left(\frac{T_l}{T}\right)\right], \qquad (3c)$$

where $\gamma$ is approximately 0.8 in Eq. (3c). By using the thermophysical parameters $\Delta T$, $C_p$, and $\Delta H_f$, the interfacial energy can be calculated.

For the $i$ phase- ($Ti_{39.5}Zr_{39.5}Ni_{21}$) and the $C14$ phase- ($Ti_{40}Zr_{30}Ni_{30}$) forming liquids, $\Delta H_f$ was determined from the total heat released during recalescence and the subsequent plateau. Fortunately, when the liquid that forms the $i$ phase is deeply undercooled, the step recalescence for the Laves phase almost disappears, simplifying the calculation of the enthalpy. The specific heat of the liquid, required for the calculation of $\Delta H_f$, was determined from the free radiative cooling curves of the sample using the Stefan-Boltzmann relation.[33] The viscosity of the equilibrium and undercooled levitated liquids was measured as a function of temperature by the oscillating droplet technique.[34]

The calculated interfacial free energies between the liquids and the three ordered nucleating phases, along with the thermodynamic parameters used, are shown in Table II for three different approximations for the driving free energy [Eq. (3)]. As expected, the interfacial free energy (0.062 J/m$^2$) for the $i$ phase is smaller than that of the Frank-Kasper polytetrahedral phase ($C14$ phase) (0.095 J/m$^2$), and the simple crystalline phase [$\beta$ phase (bcc)] (0.077 J/m$^2$). The values also compare favorably with those reported for the Al-based $i$ phase (0.09–0.11 J/m$^2$), and decagonal phase (0.11–0.16 J/m$^2$), but not for the simple crystalline phase (0.17).[12]

The smaller than expected value for the liquid/solid interfacial energy between the liquid and the $\beta$(Ti/Zr) phase seems to be inconsistent with the previous discussion regarding local structure and undercoolability. However, from Eq. (2), it reflects a smaller enthalpy of fusion for $\beta$(Ti/Zr); the nucleation barrier ($W^*$) remains larger than for the $C14$ or icosahedral phases. This illustrates that since the parameter that controls the nucleation rate is the work of cluster formation, $W^*$, Turnbull's coefficient[35] $\alpha_{LS}=\sigma_g/\Delta H_f$, where $\sigma_g = \sigma N_A{}^{1/3} V^{2/3}$, provides a better tool for evaluating undercooling data, because the enthalpy dependence is partially scaled out. For most metals, $\alpha_{LS}$ is 0.45;[2,33] Vinet *et al.*[36] found similar values of $\alpha_{LS}$ (0.468 for bcc Ti, Zr, and Hf), and 0.484 for fcc metals (Ni, Pd, Pt, Cu, Au, Ag, Ir, and Rh). Spaepen[37,38] estimated $\alpha_{LS}$ by considering the difference of configurational entropy between the bulk and the interface of the solid in the liquid:

$$\alpha_{LS} = \frac{N_i}{N}\left(\frac{\Delta S_{config}(\text{bulk}) - \Delta S_{config}(\text{interface})}{\Delta S_f}\right), \qquad (4)$$

where $N_i$ is the number of atoms in the interface, $N$ is the number of atoms in the crystal plane, $\Delta S_{config}$(bulk) is the configurational entropy of the bulk system, $\Delta S_{config}$(interface) is the configurational entropy of the interface, and $\Delta S_f$ is the fusion entropy per atom.

Holland-Moritz[12] used Eq. (4) to compute $\alpha_{LS}$ for quasicrystals and polytetrahedral crystals. The calculated $\alpha_{LS}$ values were 0.34 for the $i$ phase, and 0.39 and 0.43 for the complex crystal phases $\lambda$-$Al_{13}Fe_4$ and $\mu$-$Al_5Fe_2$, respectively. In the present case (Table II), $\alpha_{LS}$ has the smallest value (0.32) for the $i$ phase, intermediate (0.38) for the $C14$ polytetrahedral phase, and the largest (0.59) for the $\beta$(Ti/Zr) phase, consistent with the calculated values,[12] earlier experimental results,[24] and Frank's hypothesis.[3] According to Eq. (4), the smaller $\alpha_{LS}$ for the $i$ phase compared to the Laves phase indicates that the configurational entropy of the interface is closer to that of the bulk for the $i$ phase than for the Laves phase. Stated in a different way, the configuration of the liquid and solid are more similar for the $i$ phase than for the Laves phase, supporting Frank's hypothesis.[3]

The calculated work for critical cluster formation normalized by temperature ($W^*/k_BT$) is plotted in Fig. 9(a) as a function of reduced temperature for the three ordered phases; also included are the critical cluster sizes $2\sigma/\delta\mu$ [Fig. 9(b)]. At any given reduced temperature, $W^*/k_BT$ is smallest for the $i$ phase, intermediate for the Laves phase, and largest for the solid solution phase, demonstrating their relative ease of nucleation further, also in agreement with Frank's hypothesis.[3]

### C. Direct correlation between undercooling and liquid structure

That a metastable $i$ phase nucleates in preference to a stable $C14$ phase in liquids containing 21 at. % Ni (Sec. III B 2) is surprising. The driving free energy for nucleation

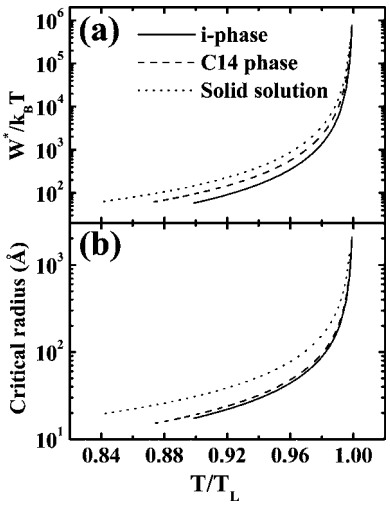


FIG. 9. (a) Calculated work for critical cluster formation and (b) critical radius for nucleation of the three phases using driving free energy expression given by by Eq. (3a).

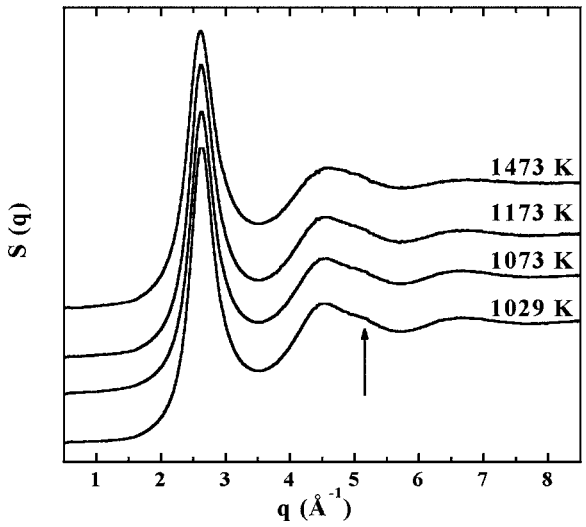


FIG. 10. $S(q)$ from a $Ti_{39.5}Zr_{39.5}Ni_{21}$ liquid as a function of temperature. The shoulder on the high-$q$ side of the second peak (indicated by the arrow) becomes more prominent as the temperature is lowered below the liquidus temperature (1083 K) (from Ref. 20).

increases with increasing $\Delta T$; at 680 °C it should be larger for the $C14$ phase ($\Delta T_{C14} \approx 140$ °C) than for the $i$ phase ($\Delta T_{i\ \mathrm{phase}} \approx 110$ °C). Further, the $i$ phase is metastable above 570 °C.[19] This unambiguously demonstrates that the $i$ phase/liquid interfacial free energy is less than that of the $C14$/liquid, *independent of particular aspects of the nucleation model* chosen for the data analysis.

The undercooling results reported here, then, provide strong support for Frank's hypothesis, but they do not prove it, since the nucleation barrier is not directly correlated with the structure of the liquid. Recently, experimental proof was obtained.[20] *In situ* high-energy x-ray diffraction studies of a $Ti_{39.5}Zr_{39.5}Ni_{21}$ (and more recently, a $Ti_{37}Zr_{42}Ni_{21}$) liquid confirmed that the primary crystallizing phase was the metastable $i$ phase. Further, diffraction studies of the supercooled liquids revealed a shoulder on the high-$q$ (momentum transfer) side of the second peak in $S(q)$ that became more prominent with undercooling (Fig. 10). The peak intensity and shoulder of this peak are sensitive to the distortions of the tetrahedral order,[39] allowing ISRO to be distinguished from regular tetrahedral short-range order. In these liquids, they match those expected for icosahedral order[40] and the second- and higher-order oscillations are well fitted by assuming that the local structure of the liquid can be described by icosahedral clusters, of the type known to occur in the structure of the icosahedral quasicrystal. Based on the classical nucleation theory, the critical cluster size for this phase (~3.45 nm at the recalescence temperature of 681 °C) is close to the coherence length of ISRO in the liquid (~2.3 nm at 720 °C), obtained from *in situ* x-ray scattering experiment.[20] The liquid, then, acts as a type of template for the nucleation of the $i$ phase.

## V. SUMMARY AND CONCLUSIONS

A systematic undercooling study has been carried out for various crystal and quasicrystal forming phases in Ti-Zr-Ni alloys. The much smaller reduced undercooling (0.09) for the $i$ phase compared to that for the polytetrahedral $C14$ Laves phase (0.14) and the simple crystalline $\beta$ phase (0.18) supports Frank's hypothesis.[3] The estimated ratios of the interfacial free energy to the enthalpy of fusion $\alpha_{LS}$ for the three phases (0.324 for the $i$ phase, 0.375 for the $C14$ Laves phase, and 0.59 for the $\beta$ phase) are consistent with theoretical expectations[12] and the undercooling behavior. This implies that the local structures of the liquid and the solid phases are more similar for the $i$ phase than for the Laves phase.

The most direct verification of Frank's hypothesis, however, comes from a direct observation of developing ISRO with increasing undercooling for the $Ti_{39.5}Zr_{39.5}Ni_{21}$ and $Ti_{37}Zr_{42}Ni_{21}$ alloy liquids, which favors the nucleation of a metastable $i$ phase instead of the stable polytetrahedral phase for these alloy compositions. Such a strong correlation between the nucleation barrier and a developing ISRO has not been established in any previous studies. These results constitute the most comprehensive data set ever obtained in a single alloy system and provide an unambiguous proof of Frank's hypothesis.

Finally, although the experimental data are reasonably well explained by the classical nucleation theory, limitations of that theory are revealed. These and previous studies[20] indicate that regions of local order spontaneously arise in the liquid. If the lifetime of the order is greater than the typical time scale for a nucleation fluctuation, they will catalyze nucleation in specific sites in space, blurring the distinction between homogeneous and heterogeneous nucleation. Further, this coupling of two different stochastic fluctuations (nucleation and ordering in the liquid) indicates that in general, nucleation cannot be described within the one-dimensional kinetic view implicit in the classical theory. A more correct treatment requires a shift to an order parameter approach, such as that incorporated in density functional treatments.[41]

**ACKNOWLEDGMENTS**

We thank Glen Fountain and Trudy L. Allen for technical assistance. The work at Washington University was supported by the National Aeronautics and Space Administration under Contracts No. NAG8-1682 and No. NNM04AA016 and the National Science Foundation under Grant No. DMR 03-07410. Work at Marshall Space Flight Center (MSFC) was supported by the Center Director's Discretionary Fund, the MSFC Science Directorate Internal Research and Development Program, and the NASA Microgravity Research Program. The use of the Advanced Photon Source was supported by the U.S. DOE, Basic Energy Sciences, Office of Science, under the Contract No. W-31-109-Eng-38, and MUCAT by Contract No. W-7405-Eng-82 through the Ames Laboratory.

*Current address: Lawrence Livermore National Laboratory, University of California, Livermore, California 94550. Electronic address: lee210@llnl.gov

[1] D. Turnbull, J. Chem. Phys. **20**, 411 (1952).
[2] K. F. Kelton, in *Solid State Physics*, edited by H. Ehrenreich and D. Turnbull (Academic Press, Boston, 1991), Vol. 45, p. 75.
[3] F. C. Frank, Proc. R. Soc. London, Ser. A **215**, 43 (1952).
[4] P. J. Steinhardt, D. R. Nelson, and M. Ronchetti, Phys. Rev. B **28**, 784 (1983).
[5] H. Jonsson and H. C. Andersen, Phys. Rev. Lett. **60**, 2295 (1988).
[6] F. Yonezawa, in *Solid State Physics*, edited by H. Ehrenreich and D. Turnbull (Academic, Boston, 1991), Vol. 45, p. 179.
[7] W.-K. Rhim, M. Collender, M. T. Hyson, W. T. Simms, and D. D. Ellemean, Rev. Sci. Instrum. **56**, 307 (1985); J. Rulison, J. L. Watkins, and B. Zambrano, *ibid.* **68**, 2856 (1997).
[8] D. M. Herlach, R. F. Cochrane, I. Egry, H. J. Fecht, and A. L. Greer, Int. Mater. Rev. **38**, 273 (1993).
[9] J. K. R. Weber, D. S. Hampton, D. R. Merkley, C. A. Rey, M. M. Zatarski, and P. C. Nordine, Rev. Sci. Instrum. **65**, 456 (1994).
[10] E. H. Trinh and K. Osaka, Int. J. Thermophys. **16**, 545 (1995).
[11] J. C. Holzer and K. F. Kelton, Acta Metall. Mater. **39**, 1833 (1991).
[12] D. Holland-Moritz, Int. J. Non-Equilib. Process. **11**, 169 (1998).
[13] C. L. Henley and V. Elser, Philos. Mag. B **53**, L59 (1986).
[14] W. Ohashi and F. Spaepen, Nature (London) **330**, 555 (1987).
[15] G. V. S. Sastry and P. Ramachandrarao, J. Mater. Res. **1**, 247 (1986).
[16] S. Ebalard, F. Spaepen, R. F. Cochrane, and A. L. Greer, Mater. Sci. Eng., A **133**, 569 (1991).
[17] D. R. Nelson and F. Spaepen, in *Solid State Physics*, edited by D. Turnbull (Academic, Boston, 1989), Vol. 42, p. 1.
[18] J. Fransaer, A. V. Wagner, and F. Spaepen, J. Appl. Phys. **87**, 1801 (2000).
[19] G. W. Lee, T. K. Croat, A. K. Gangopadhyay, and K. F. Kelton, Philos. Mag. Lett. **82**, 199 (2002).
[20] K. F. Kelton, G. W. Lee, A. K. Gangopadhyay, R. W. Hyers, T. J. Rathz, J. R. Rogers, M. B. Robinson, and D. S. Robinson, Phys. Rev. Lett. **90**, 195504 (2003).
[21] K. F. Kelton, A. K. Gangopadhyay, G. W. Lee, L. Hennet, R. W. Hyers, S. Krishnan, M. B. Robinson, J. Rogers, and T. J. Rathz, J. Non-Cryst. Solids **312–314**, 305 (2002).
[22] T. K. Croat, J. P. Davis, A. K. Gangopadhyay, K. F. Kelton, G.-W. Lee, J. M. Simmons, R. W. Hyers, M. B. Robinson, J. Rogers, and L. Savage, in *Quasicrystals–Preparation, Properties and Applications*, edited by E. Belin-Ferre, P. A. Thiel, A-P. Tsai, and K. Urban, MRS Symposia Proceedings Vol. 643 [Mater. Res. Soc. Symp. Proc. **643**, K1.3 (2001)] (Materials Research Society, Warrendale, PA, 2001).
[23] A. K. Gangopadhyay, G. W. Lee, K. F. Kelton, J. R. Rogers, T. J. Rathz, R. W. Hyers, and D. S. Robinson, Rev. Sci. Instrum. **76**, 073901 (2005).
[24] D. Holland-Moritz, J. Schroers, D. M. Herlach, B. Grushko, and K. Urban, Acta Mater. **46**, 1601 (1998).
[25] J. H. Perepezko, J. Non-Cryst. Solids **156–158**, 463 (1993).
[26] R. G. Hennig, K. F. Kelton, A. E. Carlsson, and C. L. Henley, Phys. Rev. B **67**, 134202 (2003).
[27] R. G. Hennig, E. H. Majzoub, A. E. Carlsson, K. F. Kelton, C. L. Henley, W. B. Yelon, and S. Misture, Mater. Sci. Eng., A **294–296**, 361 (2000).
[28] R. G. Hennig, Ph.D. thesis, Washington University, St. Louis, 2000 (unpublished).
[29] G. W. Lee, A. K. Gangopadhyay, K. F. Kelton, R. W. Hyers, T. J. Rathz, J. R. Rogers, D. S. Robinson, and A. I. Goldman (unpublished).
[30] R. M. Stroud, Ph.D. thesis, Washington University, St. Louis, 1996 (unpublished).
[31] C. V. Thompson and F. Spaepen, Acta Metall. **27**, 1855 (1979).
[32] L. Battezzati and E. Garrone, Z. Metallkd. **75**, 305 (1984).
[33] G. Wilde, G. P. Gorler, and R. Willnecker, Appl. Phys. Lett. **69**, 2995 (1996).
[34] R. W. Hyers, R. C. Bradshaw, J. R. Rogers, T. J. Rathz, G. W. Lee, A. K. Gangopadhyay, and K. F. Kelton, Int. J. Thermophys. **25**, 1155 (2004).
[35] D. Turnbull and R. E. Cech, J. Appl. Phys. **21**, 804 (1950).
[36] B. Vinet, L. Magnusson, H. Fredriksson, and P. J. Desre, J. Colloid Interface Sci. **255**, 363 (2002).
[37] F. Spaepen and R. Meyer, Scr. Metall. **10**, 257 (1976).
[38] F. Spaepen, Acta Metall. **23**, 729 (1975).
[39] G. W. Lee, A. K. Gangopadhyay, K. F. Kelton, R. W. Hyers, T. J. Rathz, J. R. Rogers, and D. S. Robinson, Phys. Rev. Lett. **93**, 037802 (2004).
[40] S. Sachdev and D. R. Nelson, Phys. Rev. Lett. **53**, 1947 (1984).
[41] T. V. Ramakrishnan and M. Yussouff, Phys. Rev. B **19**, 2775 (1979).